USAARL-TECH-FR--2026-36

UNITED STATES ARMY AEROMEDICAL RESEARCH LABORATORY

Preliminary Findings from an Investigation of the Influence of HSM and Inertial Loading Direction On Cervical Spine Injury Risk

Danielle Rhodes, Brandon A. Brown, Blake A. Johnson, Frederick T. Brozoski, Ray W. Daniel, Tyler F. Rooks, & Valeta Carol Chancey

Notice

Qualified Requesters

Qualified requesters may obtain copies from the Defense Technical Information Center (DTIC), Fort Belvoir, Virginia 22060. Orders will be expedited if placed through the librarian or other person designated to request documents from DTIC.

Change of Address

Organizations receiving reports from the U.S. Army Aeromedical Research Laboratory on automatic mailing lists should confirm correct address when corresponding about laboratory reports.

Disposition

Destroy this document when it is no longer needed. Do not return it to the originator.

Disclaimer

The views, opinions, and/or findings contained in this report are those of the author(s) and should not be construed as an official Department of the Army position, policy, or decision, unless so designated by other official documentation. Citation of trade names in this report does not constitute an official Department of the Army endorsement or approval of the use of such commercial items.

IRB Determination and Number

This study, USAARL 2021-09, was reviewed and approved by the USAARL Regulatory Compliance Office in accordance with USAARL Policy for research not involving human subjects and research involving post-mortem human surrogates. The study protocol was approved in January 2022.

REPORT DOCUMENTATION PAGE	*Form Approved* *OMB No. 0704-0188*

1. REPORT DATE *(DD-MM-YYYY)*: 20-08-2026

2. REPORT TYPE: Final Report

3. DATES COVERED *(From - To)*: 10/1/2022- 9/30/24

4. TITLE AND SUBTITLE

Preliminary Findings from an Investigation of the Influence of HSM and Inertial Loading Direction On Cervical Spine Injury Risk

5a. CONTRACT NUMBER

5b. GRANT NUMBER

5c. PROGRAM ELEMENT NUMBER

5d. PROJECT NUMBER: MOM21210

5e. TASK NUMBER

5f. WORK UNIT NUMBER

6. AUTHOR(S)

Rhodes, D.[1,2], Brozoski, F. T.[1], Brown, B. A.[1,2], Johnson, B. A.[1,2], Daniel, R. W.[1,3], Rooks, T. F.[1], & Chancey, V. C.[1]

7. PERFORMING ORGANIZATION NAME(S) AND ADDRESS(ES)

U.S. Army Aeromedical Research Laboratory
P.O. Box 620577
Fort Rucker, AL 36362

8. PERFORMING ORGANIZATION REPORT NUMBER: USAARL-TECH-FR--2026-36

9. SPONSORING/MONITORING AGENCY NAME(S) AND ADDRESS(ES)

U.S. Army Medical Research and Development Command
Military Operational Medicine Research Program
810 Schreider Street
Fort Detrick, MD 21702

10. SPONSOR/MONITOR'S ACRONYM(S): USAMRDC

11. SPONSOR/MONITOR'S REPORT NUMBER(S)

12. DISTRIBUTION/AVAILABILITY STATEMENT

DISTRIBUTION STATEMENT A. Approved for public release: distribution is unlimited.

13. SUPPLEMENTARY NOTES

[1]U.S. Army Aeromedical Research Laboratory; [2]Chenega Corporation; [3]Katmai Health Services

14. ABSTRACT

Current military HSM guidelines for acute injury risk are based primarily on vertical loading in a helicopter crash environment (i.e., loading in the Gz direction) (McEntire & Shanahan, 1998). Research using HSM under longitudinal (-Gx) and lateral (Gy) loadings is becoming increasingly important with future U.S. Army air and ground vehicles incorporating side-facing seats. However, no current guidelines exist for longitudinal (±Gx) inertial loadings, such as those experienced during frontal impacts, or lateral (Gy) loadings for side-facing occupants, such as those experienced during a side impact. The objective of the current study was to investigate the effects of HSM on injury severity under frontal (-Gx) and lateral (Gy) exposures. Observed injuries and kinematics measured at the junction of the seventh cervical and first thoracic vertebra (C7/T1) were documented and compared between HSM groups and loading directions, and initial qualitative impressions are presented. Future research will quantify the influence of HSM and loading direction on cervical spine injury risk.

15. SUBJECT TERMS

Acute injury, lower neck injury, lateral impact, frontal impact, Gx exposure, Gy exposure, neck injury severity

16. SECURITY CLASSIFICATION OF: a. REPORT	b. ABSTRACT	c. THIS PAGE	17. LIMITATION OF ABSTRACT	18. NUMBER OF PAGES	19a. NAME OF RESPONSIBLE PERSON
UNCLAS	UNCLAS	UNCLAS	SAR	19	Amanda Hayes, MS
					19b. TELEPHONE NUMBER *(Include area code)*: 334-255-6067

This page is intentionally blank.

Executive Summary

Military helmet systems have become increasingly complex due to the addition of night vision goggles (NVGs), communication devices, and other equipment needed by the Warfighter. The helmet and its added equipment increase the amount of mass supported by the head and neck (i.e., head-supported mass [HSM]). The increased mass has led to neck injuries not previously seen among Soldiers in an operational environment (Bass et al., 2006; McEntire & Shanahan, 1998). Current USAARL HSM guidelines for acute injury risk are based primarily on vertical loading in a helicopter crash environment (i.e., loading in the G_z direction) (McEntire & Shanahan, 1998). Research using HSM under longitudinal ($-G_x$) and lateral (G_y) loadings is becoming increasingly more relevant as future U.S. Army aviation and ground vehicles incorporate side-facing seats. No guidelines currently exist for longitudinal ($\pm G_x$) inertial loadings, such as those experienced during frontal impacts, or lateral ($\pm G_y$) loadings for side-facing occupants, such as those experienced during a side impact.

Next-generation rotary-wing aircraft, like the MV-75 Future Long Range Assault Aircraft (FLRAA), and ground vehicles are anticipated to incorporate multiple seating configurations (e.g., forward-, side-, and rear-facing) to accommodate the maximum number of occupants. The objective of the current study was to investigate the effects of HSM on injury severity under frontal ($-G_x$) and lateral (G_y) exposures. Post-mortem human subject (PMHS) head-neck complexes were subjected to inertial (frontal and lateral) loading with and without HSM using a mini-sled test system. Observed injuries and kinematics measured at the junction of the seventh cervical and first thoracic vertebra (C7/T1) were documented and compared between HSM groups and loading directions and initial qualitative impressions are presented. Future research will quantify the influence of HSM and loading direction on cervical spine injury risk.

Although a lack of specimen availability resulted in a low sample size, this study developed a methodological framework for investigating the influence of HSM and inertial loading in the lateral and frontal directions on cervical spine injury risk using upright PMHS head and neck complexes on a mini-sled. The data from the current research study can be combined with larger datasets to investigate frontal and lateral inertially induced musculoskeletal injuries. The outlined methodology and lessons learned during its development can be used to drive future studies in this area. The differences in injury outcomes between loading direction and HSM condition warrant additional work to increase the small sample size of this study and to further analyze how the risk of injury varies between loading direction and HSM condition. Additional research investigating the effects of HSM using whole-body PMHS is needed as well as research on how to limit the negative effects of rigidly coupling PMHS head and neck complexes to the sled.

This page is intentionally blank.

Table of Contents

List of Figures

Table of Contents

List of Tables

Introduction

Military helmet systems have become increasingly complex due to the addition of night vision goggles (NVGs), communication devices, and other equipment needed by the Warfighter. The helmet and the attached equipment increase the mass supported by the head and neck (i.e., head-supported mass [HSM]). The increased mass has resulted in neck injuries not previously seen among Soldiers in an operational environment (Bass et al., 2006; McEntire & Shanahan, 1998). Along with increased protection and capabilities, which are frequently necessary for military, the added helmet system mass can cause an increased risk of injury during acute exposures (Brozoski et al., 2020; McEntire & Shanahan, 1998). The added mass may also cause injuries not otherwise experienced by non-helmet wearers, particularly among Soldiers (Bass et al., 2006; McEntire & Shanahan, 1998).

Next-generation rotary-wing aircraft and ground vehicles are anticipated to incorporate multiple seating configurations (e.g., forward-, side-, and rear-facing) to accommodate the maximum number of occupants (Figure 1). For example, the Future Long Range Assault Aircraft (FLRAA), the MV-75, is a tilt rotor aircraft with side-facing seats in the main cabin. A tiltrotor aircraft with horizontal flight capabilities can shift the primary loading direction from a vertical loading direction to the horizontal plane during an impact. Depending on the seating configuration, an occupant may be subjected to longitudinal ($\pm G_x$), lateral ($\pm G_y$), or vertical ($-G_z$) accelerative loading. In addition, many currently fielded ground vehicles (e.g., M1126 Stryker Combat Vehicle) use side-facing seats. Current military HSM guidelines for acute cervical spine injury risk are based primarily on vertical loading in a helicopter crash environment (loading in the G_z direction) (McEntire & Shanahan, 1998). No current HSM guidelines exist for longitudinal ($\pm G_x$) inertial loadings, such as those experienced during frontal impacts, or lateral ($\pm G_y$) loadings experienced by side-facing occupants during frontal impacts.

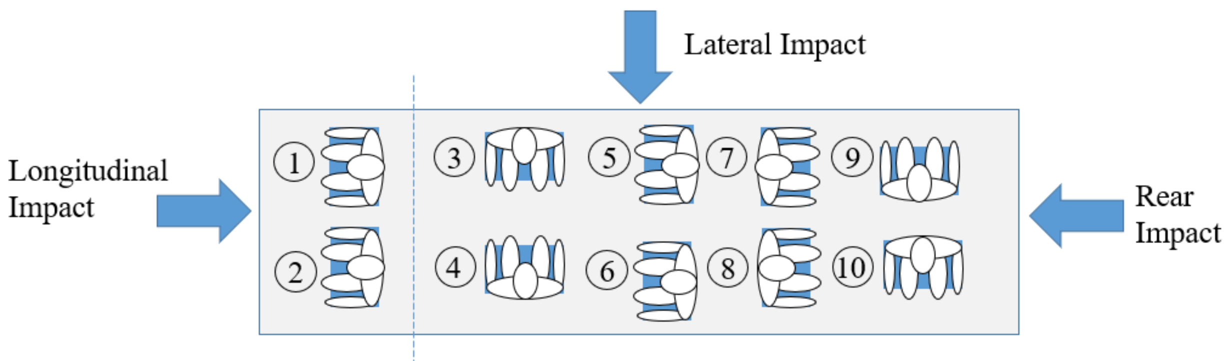

Figure 1. Seating configuration influences occupant impact direction based on vehicle impact location. For example, a frontal impact may result in either a longitudinal (i.e., anterior-posterior) impact to occupants in positions 1, 2, 5, and 6, a posterior-anterior impact to occupants in positions 5 and 6, and a lateral impact for occupants in positions 3, 4, 9, and 10.

Several military programs are requesting guidance and recommendations on HSM. The Ballistic and Blast Protection Community of Practice has identified a need for acute cervical spine injury criteria associated with HSM (Hoppel et al., 2016). Program Executive Office (PEO) Soldier is currently seeking guidance on the effects of HSM on combat helmet systems in non-aviation and aviation operating environments. The FVL Cross Functional Team (CFT) is also seeking updated medical criteria to inform advanced development of helmet-mounted systems to support new FVL platforms and improve the protection of aviation crew and passengers. Research to develop acute neck injury guidelines for a range of exposures in relevant U.S. Army operating environments with modern HSM configurations is needed to inform future materiel development and better protect the Warfighter. As such, the range of exposures must include loading from various primary directions, including longitudinal and lateral.

Since the U.S. Army Aeromedical Research Laboratory (USAARL) HSM Injury Curve was developed (McEntire & Shanahan, 1998), several new neck injury criteria (without HSM effects) have been proposed for both the upper and lower neck. Notably, many of the neck injury criteria (upper and lower) incorporate both axial force (e.g., tension or compression) and sagittal plane moment (e.g., flexion or extension) in the prediction of injury, but the effects of HSM on neck injury risk has not been thoroughly investigated (Eppinger et al., 1999; Chirvi et al., 2015, Mertz & Patrick, 1968; Prasad & Daniel, 1984; Yoganandon et al., 2020). The most widely used injury criteria for the neck (the Nij criterion developed by Kleinberger et al., 1998) incorporates both axial force and moment to predict upper neck injury risk. Although there have been significant efforts in the past to investigate upper neck injuries and associated injury criteria, investigations regarding lower neck injury risks have only occurred recently (Chirvi et al., 2015; Yoganandon et al., 2020; Kang et al., 2016; Pintar et al., 2005; Pintar, Schlick, et al., 2010; Pintar, Yoganandan, et al., 2010). One notable study developed a new injury criteria (LNij) using post-mortem human subject (PMHS) data to create a lower neck injury risk relationship (Chirvi et al., 2015). A subsequent study examined the application of the LNij to several anthropomorphic test devices (ATDs), including the Test Device for Human Occupant Restraint (THOR) and Hybrid III (HIII) (Yoganandan et al., 2020). None of the mentioned studies used HSM for the development of injury criteria or injury risk curves. In addition to recent efforts to develop lower neck injury criteria for flexion/extension motion, there are several efforts to develop and update neck injury criteria for lateral impacts (Panjabi et al., 2005; Parr et al., 2015).

There is a need to correlate acute cervical spine injury risk and HSM variables to create guidance for current and future helmet-mounted systems in order to increase the capabilities of future aviation and ground vehicle platforms. Additional research linking acute cervical spine injury risks to HSM variables in multiple loading directions is vital for advancing materiel that more effectively protects Soldiers. The objective of the current study was to investigate the effects of HSM on injury severity under frontal ($-G_x$) and lateral (G_y) exposures.

Methods

PMHS Selection and Preparation

Thirteen PMHS head and cervical spine complexes (up to the 2nd thoracic [T2] vertebral level) were evaluated for cervical spine injury patterns under frontal ($-G_x$) and lateral (G_y) loading with and without HSM. Of the thirteen specimens, three specimens were tested under a different research protocol but using similar methodology that is outlined below. All research activities complied with the U.S. Army Cadaver Policy (DoD, 2020) and were approved by the U.S. Army Medical Research and Materiel Command (now the U.S. Army Medical Research and Development Command) Office of Research and Regulatory Compliance (USAMRDC ORRC). Fresh frozen PMHS tissue was procured using the acceptance criteria specified in Table 1. Prior to specimen acceptance, a PMHS donor summary, post-mortem x-rays, and post-mortem computed tomography (CT) scans were reviewed to determine specimen acceptability for the study.

Table 1. PMHS Acceptance Criteria for Selected Specimens

PMHS Acceptance Criteria
• Males between 17 and 80 years of age
• Free of traumatic damage, fractures, or cancer that has metastasized to the bone
• With minimal spinal bridging and osteophytes
• Without existing, unhealed soft tissue injury
• No evidence of wasting disease
• Serology exams confirming no history of HIV, hepatitis B or C, COVID

Specimens were prepared by removing the surrounding soft tissues and musculature of the neck. Tissue was removed to allow the individual cervical vertebrae to be identified through palpation and observable on video while ligaments and tendons were left intact. The 1st thoracic vertebrae (T1) was covered with polymethyl methacrylate (PMMA) to improve adherence with the potting resin. After the PMMA was allowed to harden around T1, specimens were potted with the Frankfurt plane parallel to the ground and centered in a potting box, as outlined in Nightingale et al. (2004). The neck was potted in a manner that maintained the natural curvature of the cervical spine. A fast-cast isocyanate resin was poured around the PMMA to adhere the specimen to the potting box. Post potting, CT images were used to measure and confirm that the potted T1 angle was comparable with prior literature (Lee et al., 2015; Park et al., 2013).

Additional mass was added to the skull of the specimen using a triangle-shaped mounting structure for four of the seven frontal tests and four of the six lateral tests (Figure 2). The triangular fixture was affixed to the skull with screws located at the right and left lateral aspects of the calvarium 63.5 millimeters (mm) above the tragion notch and along the midcoronal plane. Based on the testing condition, weights were screwed into the triangle at pre-defined positions to achieve the desired vertical center of mass (CM) offset. Three HSM conditions were evaluated: a no HSM (no mass [NM]) condition, a high mass low offset (HMLO) condition, and a low mass high offset (LMHO) condition. The HMLO condition represented the mass moment about the tragion notch (TN) (i.e., the product of the mass and vertical CM offset relative to the TN) of an Advanced Combat Helmet (ACH) with night vision goggles and included a 3.27 kilogram (kg) added mass that was longitudinally aligned with and located 34.9 mm above the TN. The LMHO condition, which represented the mass moment about the TN of an ACH with no attachments, included a 1.46 kg mass that was longitudinally aligned with and located 76.2 mm above the TN (Figure 3). The HMLO and LMHO HSM conditions replicated the HSM properties of fielded helmets that fell outside the region of acceptable risk specified (Figure 3) by the USAARL HSM Injury Curve (McEntire & Shanahan, 1998).

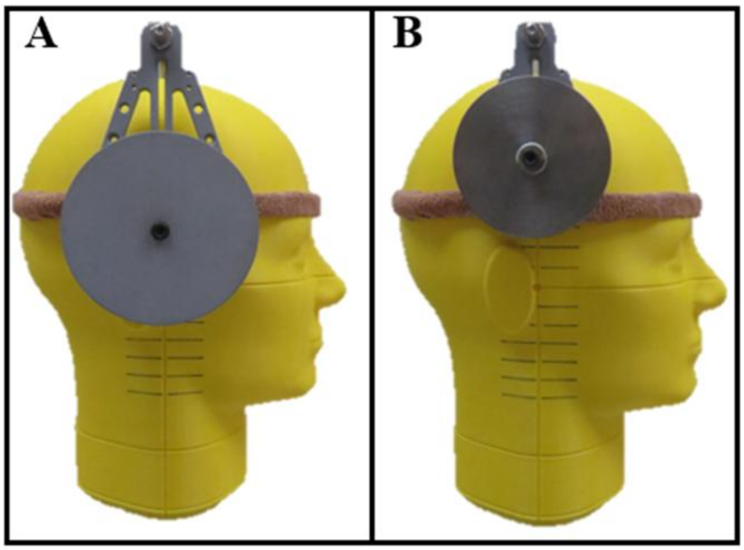

Figure 2. A custom triangle fixture rigidly coupled to the PMHS skull allowed consistent attachment and location of HSM conditions for all PMHS specimens. The custom triangle fixture is shown attached via a headband to a 3D printed headform (Flath et al., 2020) to represent the PMHS used in the study. The [A] high mass low offset (HMLO) and [B] low mass high offset (LMHO) conditions are shown.

This space is intentionally blank.

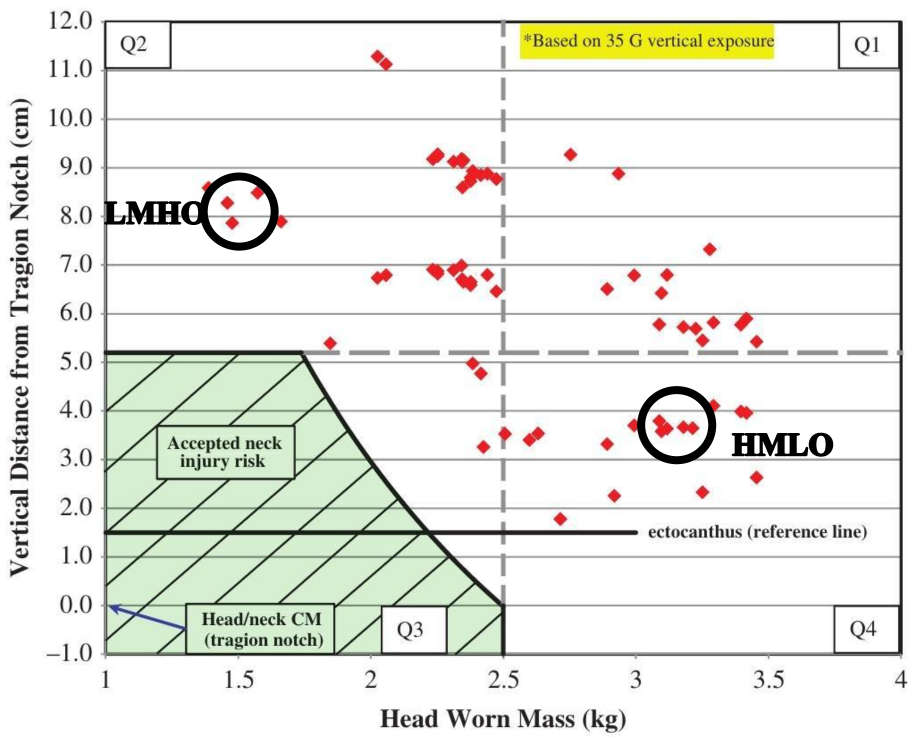

Figure 3. The USAARL HSM Injury Curve (McEntire & Shanahan, 1998) is shown with data points of currently fielded HSM configurations represented by red diamonds (figure adapted from Estep et al., 2019). The black circles indicate the targeted areas of interest for the current study, including the HMLO and LMHO HSM conditions.

The potting box was mounted on a lower neck load cell from a HIII 50th percentile male (50M) ATD (Model 1794AJLN2, The Humanetics Group, Farmington Hills, MI) to capture forces and moments at the base of the neck (C7/T1). The load cell measured three axes of force and three axes of moment. The first three PMHS were instrumented with a six-degree-of-freedom (6-DOF) accelerometer, measuring three axes of acceleration and three axes of angular rate, attached to the left temple of the specimen. Subsequent PMHS were instrumented with a 6-DOF accelerometer block attached to the palate of the specimen using dental cement. The orientations of the 6-DOF accelerometer blocks and their positions relative to the head center of gravity (CG) were identified via pre-test CT scans. Additionally, three accelerometers were rigidly attached to the front of the potting box to measure acceleration in the primary axes of motion (Figure 4). During the tests using the triangular fixture for the HSM conditions, three additional accelerometers were attached to the left triangle for frontal impacts and the right triangle for lateral impacts to measure acceleration in each of the primary axes. Researchers added padding during lateral exposures to eliminate any secondary direct impacts in the event of a potting failure or neck disarticulation for both exposure directions (only illustrated in Figure 4B).

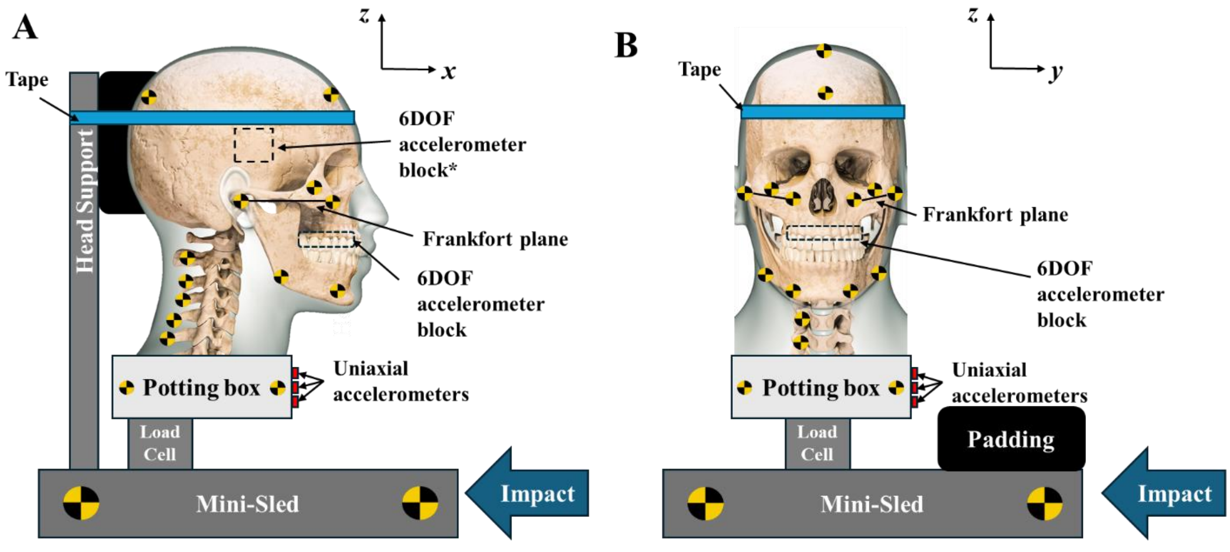

Figure 4. The USAARL mini-sled was configured with a custom setup for PMHS testing under (A) frontal and (B) lateral inertial loading conditions with the pendulum impacting the sled on the right side of the image. The setup included a support structure to ensure proper PMHS head-neck specimen positioning while mounted on the mini-sled. Padding (shown with the lateral test condition) was added to eliminate any secondary direct impacts in the event of a potting failure or neck disarticulation. Note. The first three PMHS from the previous frontal impact study were instrumented with a 6-DOF accelerometer block at the left temple of the specimen.

Fiducial markers were placed on the cervical spine and skull of each specimen. For frontal impacts, cervical spine marker pins were inserted into the spinous process at multiple levels from T1 to C2. Additional markers were placed in the right infraorbital foramen, right mandibular foramen, right mandibular angle, right zygomatic arch, anterior and posterior aspects of the calvarium along the midsagittal plane, and left and right lateral aspects of the calvarium along the midcoronal plane (Figure 4A). For lateral impacts, cervical spine marker pins were inserted into the right lateral surface of vertebral bodies at multiple levels T1 to C2. Additional markers were placed in the left and right infraorbital foramen, left and right mandibular foramen, left and right mandibular angle, left and right zygomatic arch, anterior and posterior aspects of the calvarium along the midsagittal plane, and left and right lateral aspects of the calvarium along the midcoronal plane (Figure 4B).

Experimental Design and Testing

The USAARL mini-sled test device was used to provide the indirect (inertial) loading on the specimen. Sled components included a low friction sled placed on a 3.66 meter (m) horizontal rail. Specimens were mounted upright to the USAARL mini-sled, and an inertial load was applied by a pendulum impacting the sled (Rooks et al., 2018). A load cell was also attached at the end of the pendulum to measure the load delivered to the mini-sled. The specimens were mounted appropriately for the loading direction (frontal or lateral) and positioned so that the Frankfort plane was parallel to the ground. Specimens were then secured against a head support structure with blue masking tape to hold the specimen in place until impact (Figure 4). The head coordinate system, with its origin at the head CG, was aligned with the global coordinate system prior to impact.

The PMHS responses under frontal ($-G_x$) and lateral (G_y) loading were evaluated. Frontal loading involved the pendulum striking the sled parallel to the *x*-axis of the head (Figure 4A), resulting in an impact to the front side of the specimen (i.e., $-G_x$). Lateral loading involved the pendulum striking the sled parallel to the *y*-axis of the head (Figure 4B), resulting in an impact to the left side of the specimen (G_y).

Three HSM conditions were tested: baseline (i.e., NM), LMHO, and HMLO. The frontal NM tests ($n = 3$) were conducted under an earlier test series that used a target sled velocity of 3.5 meters per second (m/s). These specimens were included in the study to increase the study sample size as there were PMHS availability issues caused by the COVID-19 pandemic. Based on the observed injury patterns from the three NM tests, all remaining frontal tests were conducted at a lower target velocity of 2.5 m/s. As no prior research was identified for lateral exposures to the head-neck complex, the first lateral NM test was conducted at the lowest achievable target velocity of 1.4 m/s to evaluate the test setup. All remaining lateral tests were conducted at 2.5 m/s, which was the same target velocity as the frontal HSM tests (Table 2).

Table 2. Number of Specimens Tested Within Each Experimental Condition

Loading Direction	**HSM Condition**	**Number of Specimens**	**Severity (Target Sled Velocity)**
Frontal ($-G_x$)	NM+	3	High (3.5 m/s)
	HMLO	2	Medium (2.5 m/s)
	LMHO	2	Medium (2.5 m/s)
Lateral (G_y)	NM	1	Low (1.4 m/s)
	NM	1	Medium (2.5 m/s)
	HMLO	2	Medium (2.5 m/s)
	LMHO	2	Medium (2.5 m/s)

+Data from a different test series.

To perform a test, the sled was positioned at the end of the track and accelerated by the impact of a 45.4 kg pendulum. By varying the pendulum release height and interface with the sled, the acceleration pulse could be tuned for the specific test conditions (energy, shape, sled velocity, and duration) (Rooks et al., 2018). Immediately prior to releasing the pendulum, the blue masking tape was pre-cut to 50% of its width, reducing the load required to break the tape and minimizing the potential for affecting the study results. Afterward, the pendulum was released from the preset release height and allowed to impact the sled, inducing the inertial exposure.

All electronic sensor data were collected at 20,000 samples per second using a Synergy 8 data acquisition system (Hi-Techniques, Madison, WI). Fiducial marker movement was captured throughout the test via overhead and lateral view high-speed video cameras. The overhead camera, Phantom VEO (Vision Research Inc., Wayne NJ), and lateral view camera, Phantom Miro (Vision Research Inc., Wayne NJ), were set to capture images at 2,000 frames per second. All data collection was time synced and triggered using the pendulum release switch.

Data Analysis

Measured accelerations, angular rates, forces, and moments were filtered at Channel Frequency Class 60 (SAE International, 2022). Head accelerations and angular rates were translated to the head CG via rigid body kinematics using the relative position of the sensors to the head CG combined with the linear and rotational motion of the head. The head CG position of each specimen was extracted from subject-specific 3D models of medical imaging and known tissue properties using Mimics software (Materialise Leuven, Belgium) (Roush, 2010). Lower neck load cell data were inertially compensated and translated to the midline of the anterior-superior edge of the T1 vertebral body from the load cell between the sled and the potting box.

Post-test autopsies were conducted to document the resulting injuries. Injuries and fractures were recorded and documented photographically, with injury type and severity graded in accordance with the Abbreviated Injury Scale (AIS) (Gennarelli & Wodzin, 2006). Observed injuries were compared to determine differences between loading and injury patterns for all combinations of HSM conditions and loading directions.

This space is intentionally blank.

Results

Specimen Demographics

Demographics of each specimen, as they are provided by the procurement service, are reported in Table 3. Averages and standard deviations (SD) for the demographic variables are provided in Table 3 for the subsets of specimens used in frontal and lateral exposures, as well as for all specimens involved in the study. Specimens 1 through 7 were used in the frontal impact tests, and specimens 8 through 13 were used in the lateral impact tests.

Table 3. Demographics for the PMHS Specimens

Spec. #	HSM Condition	Test Orientation	Age (yrs)	Height (in)	Weight (lb)	BMI (lb/in^2)	Cause of Death
1	Null	-Gx	63	74	150	19.3	Non-Hodgkin's lymphoma
2	Null	-Gx	76	69	186	27.5	Colon cancer
3	Null	-Gx	76	67	124	19.4	Parkinson's disease
4	HMLO	-Gx	76	67	154	24.1	Respiratory failure, sepsis
5	HMLO	-Gx	78	73	155	20.4	Metastatic adenocarcinoma of lung
6	LMHO	-Gx	80	72	190	25.8	Acute myelogenous leukemia
7	LMHO	-Gx	77	71	130	18.1	Cardiopulmonary arrest, Hypercapnia
Frontal Specimen Average			75.1	70.4	155.6	22.1	
Frontal Specimen SD			± 5.1	± 2.6	± 23.3	± 3.4	
8	Null	Gy	74	68	150	22.8	Colon cancer
9	Null	Gy	73	69	168	24.8	Colon cancer
10	HMLO	Gy	38	70	130	18.7	Lung cancer
11	HMLO	Gy	79	76	250	30.4	Sepsis, urinary tract infection, prostate cancer
12	LMHO	Gy	75	70	130	18.7	Alzheimer's disease, chronic obstructive lung disease
13	LMHO	Gy	71	67	150	23.5	Coronary artery disease, Peripheral arterial disease, Type 2 diabetes
Lateral Specimen Average			68.3	70.0	163.0	23.2	
Lateral Specimen SD			± 13.8	± 2.9	± 41.0	± 4.0	
Combined Specimen Average			72.0	65.7	149.7	21.3	
Combined Specimen SD			± 19.5	± 17.1	± 45.6	± 5.9	

Frontal Impact Tests

Seven male PMHS specimens were tested under frontal (-G_x) impacts. Specimens 1 through 3 were a part of a previous study that used a faster sled velocity than tests involving HSM conditions. In the NM condition, peak sled velocity was 3.46 m/s (± 0.02 m/s) on average, which resulted in peak head resultant linear acceleration of 17.80 G (± 4.5 G) and peak head angular rate of 24.4 rad/s (± 3.2 rad/s) on average. Average force measured at C7/T1 was 447.1 N (± 57.2 N) and 449.7 N (± 113.0 N) in the shear and axial directions, respectively. The moment measured at C7/T1 was 26.9 Nm (± 3.4 Nm) on average (Table 4).

Two specimens (specimens 4 and 5) were tested in the HMLO condition. In the HMLO condition, peak sled velocity was 2.65 m/s (± 0.02 m/s) on average, which resulted in peak head resultant linear acceleration of 8.7 G; acceleration data were only collected for specimen 4 due to a sensor failure on specimen 5. The peak head angular rate was 23.7 rad/s (± 0.3 rad/s) on average. Average force measured at C7/T1 was 455.3 N (± 22.4 N) and 563.4 N (± 11.8 N) in the shear and axial directions, respectively. The moment measured at C7/T1 was 33.9 Nm (± 0.0 Nm) on average (Table 4).

Two specimens (specimens 6 and 7) were tested in the LMHO condition. In the LMHO condition, peak sled velocity was 2.69 m/s (± 0.06 m/s) on average, which resulted in peak head resultant linear acceleration of 12.9 G (± 1.3 G), and peak head angular rate of 21.0 rad/s (± 0.3 rad/s) on average. Average force measured at C7/T1 was 329.3 N (± 82.4 N) and 520.9 N (± 44.7 N) in the shear and axial directions respectively. The moment measured at C7/T1 was 31.0 Nm (± 0.6 Nm) on average (Table 4).

Table 4. Head-Supported Mass (HSM), Sled Velocity, Head Kinematics, and C7/T1 Forces and Moments for Each Specimen Tested in the Frontal (-G_x) Direction

Spec. #	Direction	HSM	Sled Velocity (m/s)	Head Resultant Acceleration (G)	Head Angular Rate (rad/s)	C7/T1 Shear Force (N)	C7/T1 Axial Force (N)	C7/T1 Moment (Nm)*	Injury Occurred
1	**-Gx**	**NM**	3.48	19.2	26.9	468.4	598.6	31.3	yes
2	**-Gx**	**NM**	3.48	22.5	26.4	504.1	425.5	23	no
3	**-Gx**	**NM**	3.43	11.7	19.8	368.9	325	26.5	yes
Avg	**-Gx**	**NM**	3.46	17.8	24.4	447.1	449.7	26.9	
SD	**-Gx**	**NM**	± 0.02	± 4.5	± 3.2	± 57.2	± 113.0	± 3.4	
4	**-Gx**	**HMLO**	2.67	8.7	23.9	477.6	575.1	33.9	yes
5	**-Gx**	**HMLO**	2.62	NA	23.4	432.9	551.6	33.9	yes
Avg	**-Gx**	**HMLO**	2.65	8.7	23.7	455.3	563.4	33.9	
SD	**-Gx**	**HMLO**	± 0.02	± 0.0	± 0.3	± 22.4	± 11.8	± 0.0	
6	**-Gx**	**LMHO**	2.74	14.1	21.3	411.6	476.2	31.6	no
7	**-Gx**	**LMHO**	2.63	11.6	20.7	246.9	565.5	30.4	yes
Avg	**-Gx**	**LMHO**	2.69	12.9	21.0	329.3	520.9	31.0	
SD	**-Gx**	**LMHO**	± 0.06	± 1.3	± 0.3	± 82.4	± 44.7	± 0.6	

Note. NM - No added HSM, HMLO - Added HSM with high mass and low offset, LMHO - Added HSM with low mass and high offset, *Frontal - about Y axis, NA - Not captured due to sensor failure, Avg - average value, SD - Standard deviation

Injuries were found in two out of the three specimens tested (specimens 1 and 3) in the NM condition (Table 5). Both injured specimens sustained a complete dislocation at C7/T1 with all posterior ligaments torn; these injuries were assessed as AIS 5 in severity. The specimens tested in the HMLO condition were both injured (specimen 4 and 5). Specimen 4 sustained a fracture at the 6th cervical vertebrae (C6) with an interspinal ligament tear which resulted in a maximum AIS of 2. Specimen 5 sustained identical injuries as specimens 1 and 2. One of the two specimens exposed to the LMHO conditions (specimen 7) sustained a fracture of the 4th cervical vertebrae (C4) and a ruptured joint capsule at C4/C5 resulting in a maximum AIS of 2.

Table 5. Documented PMHS Injuries for Frontal ($-G_x$) Tests

Specimen #	**HSM**	**Injury Description**	**Max AIS Score**
1	NM	Complete dislocation at C7/T1; all posterior ligaments suffered a complete tear	5
2	NM	No injuries	NA
3	NM	Complete dislocation at C7/T1; all posterior ligaments suffered a complete tear	5
4	HMLO	C6 fracture; interspinal ligament tear	2
5	HMLO	Complete dislocation at C7/T1; all posterior ligaments suffered a complete tear	5
6	LMHO	No injuries	NA
7	LMHO	C4 spinous process fracture; C4/5th cervical vertebra (C5) joint capsule separated	2

This space is intentionally blank.

Lateral Impact Tests

Six male PMHS specimens were tested under lateral (G_y) impacts. In the NM condition, specimen 8 was tested under a lower peak sled velocity than specimen 9. Average peak sled velocity in the NM condition was 2.0 m/s (± 0.58 m/s), which resulted in peak head resultant linear acceleration of 6.0 G (± 2.7 G) and peak head angular rate of -13.8 rad/s (± 6.6 rad/s) on average. Average force measured at C7/T1 was 152.0 N (± 47.5 N) and 169.3 N (± 117.5 N) in the shear and axial directions, respectively. The moment measured at C7/T1 was -15.6 Nm (± 9.0 Nm) on average (Table 6).

Two specimens (specimens 10 and 11) were tested in the HMLO condition. In the HMLO condition, peak sled velocity was 2.41 m/s (± 0.01 m/s) on average, which resulted in peak head resultant linear acceleration of 5.3 G (± 0.5 G), and peak head angular rate of -17.8 rad/s (± 1.8 rad/s) on average. Average force measured at C7/T1 was 407.4 N (± 2.6 N) and 249.5 N (± 73.4 N) in the shear and axial directions, respectively. The moment measured at C7/T1 was -46.4 Nm (± 2.0 Nm) on average (Table 6).

Two specimens (specimens 12 and 13) were tested in the LMHO condition. In the LMHO condition, peak sled velocity was 2.49 m/s (± 0.01 m/s) on average, which resulted in peak head resultant linear acceleration of 6.5 G (± 0.4 G), and peak head angular rate of -20.2 rad/s (± 0.1 rad/s) on average. Average force measured at C7/T1 was 269.7 N (± 18.9 N) and 180.8 N (± 29.3 N) in the shear and axial directions, respectively. The moment measured at C7/T1 was -29.3 Nm (± 0.2 Nm) on average (Table 6).

Table 6. HSM, Sled Velocity, Head Kinematics, and C7/T1 Forces and Moments for Each Specimen Tested in the Lateral (G_y) Direction.

Spec. #	Direction	HSM	Sled Velocity (m/s)	Head Resultant Acceleration (G)	Head Angular Rate* (rad/s)	C7/T1 Shear Force (N)	C7/T1 Axial Force (N)	C7/T1 Moment (Nm)*	Injury Occurred
8	**Gy**	**NM**	1.42	3.3	-7.2	104.5	51.8	-6.6	no
9	**Gy**	**NM**	2.58	8.6	-20.4	199.5	286.7	-24.6	yes
Avg	**Gy**	**NM**	2.00	6.0	-13.8	152.0	169.3	-15.6	
SD	**Gy**	**NM**	± 0.58	± 2.7	± 6.6	± 47.5	± 117.5	± 9.0	
10	**Gy**	**HMLO**	2.42	4.8	-19.6	409.9	176.1	-48.3	yes
11	**Gy**	**HMLO**	2.39	5.8	-16	404.8	322.9	-44.4	yes
Avg	**Gy**	**HMLO**	2.41	5.3	-17.8	407.4	249.5	-46.4	
SD	**Gy**	**HMLO**	± 0.01	± 0.5	± 1.8	± 2.6	± 73.4	± 2.0	
12	**Gy**	**LMHO**	2.5	6.1	-20.2	250.8	151.5	-29.1	yes
13	**Gy**	**LMHO**	2.47	6.9	-20.1	288.6	210.0	-29.4	yes
Avg	**Gy**	**LMHO**	2.49	6.5	-20.2	269.7	180.8	-29.3	
SD	**Gy**	**LMHO**	± 0.01	± 0.4	± 0.1	± 18.9	± 29.3	± 0.2	

Note. NM - No added HSM, HMLO - Added HSM with high mass and low offset, LMHO - Added HSM with low mass and high offset, *Lateral - about *x*-axis, Avg - average value, SD - Standard deviation

Specimens 8 and 9 were tested in the NM condition. Specimen 8 was tested at the lowest sled velocity among all tests in the lateral configuration and did not sustain any injuries (Table 7). When the sled velocity was increased, specimen 9 sustained a C7/T1 dislocation with spinal cord involvement and a partial C3/C4 dislocation with a maximum AIS of 3. Each of the last four specimens tested in the lateral configuration sustained an injury. A single specimen from each HSM condition (specimens 10 and 13) sustained injuries resulting in a maximum AIS of 5. Specimen 11, which was tested in the HMLO configuration, sustained a single facet capsule rupture between C6 and C7. Specimen 12 was tested in the LMHO configuration and sustained a single spinal interspinous ligament rupture between C3 and C4.

Table 7. Documented PMHS Injuries for Lateral (G_y) Tests

Specimen	Test	Injury Description	Max AIS Score
8	NM	No injuries	NA
9	NM	C7/T1 dislocation with spinal cord involvement; partial C3/C4 dislocation	3
10	HMLO	First cervical vertebra (C1) superior facet fracture; interspinous ligament rupture between second cervical vertebra (C2) /C3; ruptured spinal cord at C2/C3; C7/T1 dislocation	5
11	HMLO	C6/C7 right facet capsule rupture	2
12	LMHO	Interspinous ligament rupture between C3/C4	1
13	LMHO	C1/C2 right facet capsule rupture; right C6/C7 facet capsule rupture, left C3/C4 facet capsule rupture; left C4/C5 facet capsule rupture; complete C7/T1 dislocation	5

This space is intentionally blank.

Discussion

The objective of the current study was to investigate the effects of HSM on injury severity under frontal ($-G_x$) and lateral (G_y) inertial exposures using PMHS head-neck complexes. Due to project constraints that involved low specimen availability, resulting from the COVID-19 pandemic, data from specimens tested under frontal exposures in the NM condition under a previously conducted study were included. The additional data included specimens tested at a higher sled velocity and instrumented with a 6-DOF block mounted to the side of the skull instead of the palate. The 6-DOF mounting location was not anticipated to introduce any confounding errors.

This study developed a methodological framework to investigate the influence of HSM and lateral and frontal inertial loading directions on cervical spine injury risk using upright PMHS head and neck complexes mounted to a mini-sled. Additionally, the study delivered initial results toward developing cervical spine injury risk curves for frontal and lateral inertial loading directions. Throughout study execution, there were notable lessons learned. The first being that rigidly mounting added mass to the skull minimizes extraneous motion of the HSM fixture. The second being that the removal of soft tissue and musculature can place the head and neck outside the plausible range of motion in the event of cervical neck tissue failure during testing. A third notable lesson learned was that adding a pad to the sled system for frontal and lateral test exposures can eliminate any secondary direct impacts in the event of a potting failure or neck disarticulation.

Limited sample size prevented the ability to make statistical deductions regarding trends observed between the different mass conditions and loading directions. However, qualitative observational comparisons between the sustained injuries were able to be made. In the frontal loading condition, specimens tested with added mass sustained similar injuries to specimens tested with no added mass but a higher sled velocity (Table 4). The injury similarities between mass conditions with different loading rates can be attributed to the HSM adding more stress to the cervical spine throughout the inertial loading event, which demonstrates a potential increase in cervical spine injury risk due to the HSM. Specimens tested in the lateral loading condition with HSM sustained injuries of similar severity as specimens tested in the frontal loading condition, which can indicate that lateral inertial loading has at least the same cervical neck injury potential as frontal inertial loading. Furthermore, specimens tested with HSM in both loading directions were observed to sustain injuries further up the cervical spine than in the NM condition. Since T1 is rigidly fixed to the potting box, the C7/T1 motion segment is expected to experience the largest bending moment and likely to be the location of a resulting injury. The observation of added mass resulting in injuries further up the cervical spine could be indicative of a change in injury potential and highlights the importance of continued HSM research.

Several prior studies have investigated the effects of inertial lateral loading with and without HSM; however, many of the studies used live subjects, and the results are not comparable with the current study. There is a limited amount of literature outlining inertial lateral loading on PMHS specimens without HSM (Bendjellal et al., 1987; Horsch et al., 1979; Kallieris et al., 1987; Kallieris & Schmidt, 1990; Kallieris et al., 1991; Philippens et al., 2011). These tests used whole-body PMHS to investigate automotive and aircraft side-impact injuries. The exposure velocities for these studies ranged from 6 to 18 m/s at the seat (no estimate of the

C7/T1 velocity was provided for comparison with the current work). Most reported injuries were AIS 3 or lower; AIS level 5 injuries were relatively uncommon and occurred at seat velocities of at least 8.33 m/s. In contrast, the present study, which used head-neck complexes and included HSM, resulted in two out of the five specimens sustaining AIS 5 injuries at C7/T1 when tested at a sled velocity of 2.47 m/s. The differences in injury outcomes may be due to differences in the experimental setup, including our use of head-neck complexes versus whole-body PMHS, as well as the inclusion of HSM.

Limitations

Three primary limitations exist in this study. First, older specimens were used and may not be indicative of the military population. Age-related spinal degeneration is commonly observed among the PMHS population, but specimens with spinal degeneration generally are screened during the selection process. However, due to limited PMHS availability, there were specimens with osteophyte bridging between vertebrae of the neck present in this study. It is possible that osteophyte bridging may have influenced the kinematic differences observed between test conditions. The differences in head angular rate between specimens of the same HSM condition could also be due to poor neck flexibility caused by osteophyte bridging. For example, Specimen 9, despite having no HSM, sustained similar injuries as specimens 10 and 13 being exposed to similar sled velocities in lateral testing (Table 6). Specimen 9 had osteophytes at C6/C7 that likely affected the ROM and thus was more susceptible to injury.

The second limitation of the current study is its low sample size. Due to the low number of specimens, statistical conclusions were not able to be made, and additional testing is needed to fully understand the relationship between HSM, injury, and kinematic and kinetic responses.

The third potential limitation is the possibility that the rigid coupling of the neck to the sled contributed to the dislocations observed in the lower neck. While rigid coupling of the neck to the sled may have contributed to the observed injuries, prior research using whole-body PMHS specimens demonstrated that a specimen’s torso movement must be minimized to produce the head-neck response necessary for injury (Philippens et al., 2011). For lateral impacts, several of the tests with HSM sustained middle and upper spinal ruptures and dislocations. Injuries in the middle to upper neck would not be as affected by the rigid coupling as vertebrae in the lower cervical spine. Potting the specimens at a vertebra lower than C7/T1 (similar to prior work by Bass et al. [2006] and Kang et al. [2016]) may result in more realistic injury outcomes. Further, testing with whole-body PMHS specimens may also result in more realistic injury outcomes; however, the test-to-test variability in whole-body PMHS tests may limit findings specific to the role of HSM in the risk of injury. Additional research investigating methods to reproduce a small amount of compliance at the C7/T1 boundary in head-neck complex tests is needed.

This space is intentionally blank.

Conclusion

Research using HSM under longitudinal (-Gx) and lateral (Gy) loadings is becoming increasingly important with future U.S. Army aviation and ground vehicles incorporating side-facing seats. Although a lack of specimen availability resulted in low sample size, this study developed a methodological framework for investigating the influence of HSM and lateral and frontal inertial loading directions on cervical spine injury risk using upright PMHS head and neck complexes mounted to a mini-sled. The data from the current research study can be combined with larger datasets to investigate frontal and lateral inertially-induced musculoskeletal injuries. The methodology and lessons learned during its development can be used to drive future studies in this area. The differences in injury outcomes between loading direction and HSM condition warrant additional work to increase the small sample size of this study and to further analyze how the risk of injury varies between loading direction and HSM condition. Additional research investigating the effects of HSM using whole-body PMHS is needed as well as research on how to limit the negative effects of rigidly coupling PMHS head and neck complexes to the sled.

References

Bass, C. R., Donnellan, L., Salzar, R., Lucas, S., Folk, B., Davis, M., Rafaels, K., Planchak, C., Meyerhoff, K., & Ziemba, A. (2006). A new neck injury criterion in combined vertical/frontal crashes with head supported mass. *In Proceedings of the IRCOBI Conference, Madrid, Spain* (pp. 20–22). https://www.ircobi.org/wordpress/downloads/irc0111/2006/Session2/21.pdf

Bendjellal, F., Terriere, C., Gillet, D., Mack, P., & Guillon, F. (1987). Head and neck responses under high G-level lateral deceleration. *SAE Transactions, 96*(3), 1336–1354. https://www.jstor.org/stable/44472896

Brozoski, F. T., Chancey, V. C., Licina, J. R., & McEntire, B. J. (2020). *Retrospective review of spinal injuries in US Army rotary-wing mishaps: January 1990-December 2014* (Report No. USAARL-TECH-FR--2020-024). U.S. Army Aeromedical Research Laboratory. https://apps.dtic.mil/sti/pdfs/AD1104501.pdf

Chirvi, S., Pintar, F. A., & Yoganandan, N. (2015). An examination of isolated and interaction-based biomechanical metrics for potential lower neck injury criteria. *In ASME International Mechanical Engineering Congress and Exposition* (pp. V003T03A060). American Society of Mechanical Engineers. https://doi.org/10.1115/IMECE2015-52108

DoD. (2020). *Army policy for use of human cadavers for research, development, and evaluations [RDT&E], education or training.* Secretary of the Army, Department of Defense.

Eppinger, R., Sun, E., Bandak, F., Haffner, M., Khaewpong, N., Kuppa, S., Maltese, M., Kuppa, S., Nguyen, T., Takhounts, E., Tannous, R., & Zhang, A. (1999). *Development of improved injury criteria for the assessment of advanced automotive restraint systems: II.* National Highway Traffic Safety Administration. https://rosap.ntl.bts.gov/view/dot/14738

Estep, P. N., Bonts, E. G., Shivers, B. L., Wurzbach, J. M., Novotny, B. L., Rybarczyk, K., & Chancey, V. C. (2019). Mass properties comparison of dismounted and ground-mounted head-supported mass configurations to existing performance and acute injury risk guidelines. *Military Medicine*, *184*(Supplement_1), 245–250.

Flath, N. L., McEntire, B. J., & Carboni, M. (2020). *Proposed standard for measuring head-supported mass properties* (Report No. USAARL-TECH-TR--2020-052). U.S. Army Aeromedical Research Laboratory. https://apps.dtic.mil/sti/trecms/pdf/AD1111116.pdf

Gennarelli, T. A., & Wodzin, E. (2006). AIS 2005: A contemporary injury scale. *Injury, 37*(12), 1083–1091.

Hoppel C., Colanto, D., DiLalla, R., Fontecchio, J., Fournier, A., Kimball, B., Kirejczyk, J., Markey, M., McEntire, B.J., Mullenix, J., Phelps, D., Satapathy, S., Vargas-Gonzalez, L., & Wetzel, E. (2016). *Ballistic and blast protection 2016 research goals* (Report No. TR-16/026L). Natick, MA.

Horsch, J. D., Schneider, D. C., Kroell, C. K., & Raasch, F. D. (1979). Response of belt restrained subjects in simulated lateral impact. *SAE Transactions, 88*(4), 3338–3357. https://www.jstor.org/stable/44648334

Kallieris, D., Schmidt, G., & Mattern, R. (1987). Vertebral column injuries in 90-degrees collisions. A study with post-mortem human objects. *In Proceedings of the IRCOBI Conference*, Birmingham, UK (pp. 189– 202). https://www.ircobi.org/wordpress/downloads/irc1987/pdf_files/1987_15.pdf

Kallieris, D., & Schmidt, G. (1990). Neck response and injury assessment using cadavers and the US-SID for far-side lateral impacts of rear seat occupants with inboard-anchored shoulder belts. *SAE Transactions, 99*(6), 1709–1716. https://www.jstor.org/stable/44554109

Kallieris, D., Mattern, R., Miltner, E., Schmidt, G., & Stein, K. (1991). Considerations for a neck injury criterion. *SAE Transactions, 100*(6), 2049–2065. https://www.jstor.org/stable/44632175

Kang, Y. S., Stammen, J., Moorhouse, K., Herriott, R., & Bolte, J. H. (2016). PMHS lower neck load calculation using inverse dynamics with cervical spine kinematics and neck mass properties. *In Proceedings of the IRCOBI Conference*, Malaga, Spain (pp. 14–16). https://www.ircobi.org/wordpress/downloads/irc16/pdf-files/25.pdf

Kleinberger, M., Sun, E., Eppinger, R., Kuppa, S., & Saul, R. (1998). Development of improved injury criteria for the assessment of advanced automotive restraint systems. *NHTSA Docket, 4405*(9), 18–32. https://www.nhtsa.gov/sites/nhtsa.gov/files/criteria_0.pdf

Lee, S. H., Son, E. S., Seo, E. M., Suk, K. S., & Kim, K. T. (2015). Factors determining cervical spine sagittal balance in asymptomatic adults: correlation with spinopelvic balance and thoracic inlet alignment. *The Spine Journal*, *15*(4), 705–712. https://doi.org/10.1016/j.spinee.2013.06.059

McEntire, B. J., & Shanahan, D. F. (1998). *Mass requirements for helicopter aircrew helmets* (Report No. 98-14). U.S. Army Aeromedical Research Laboratory. https://usaarl.health.mil/assets/docs/techReports/98-14.PDF

Mertz, H. J., & Patrick, L. M. (1968). Investigation of the kinematics and kinetics of whiplash. *SAE Transactions, 76*, 2952–2980. http://www.jstor.org/stable/44562840

Nightingale, R. W., Chancey, V. C., Luck, J. F., Tran, L., Ottaviano, D., & Myers, B. S. (2004). The human cervical spine in tension: Effects of frame and fixation compliance on structural responses. *Traffic Injury Prevention*, *5*(2), 151–155. https://www.tandfonline.com/doi/full/10.1080/15389580490435213

Panjabi, M. M., Ivancic, P. C., Tominaga, Y., & Wang, J. L. (2005). Intervertebral neck injury criterion for prediction of multiplanar cervical spine injury due to side impacts. *Traffic Injury Prevention*, *6*(4), 387–397.

Park, J. H., Cho, C. B., Song, J. H., Kim, S. W., Ha, Y., & Oh, J. K. (2013). T1 slope and cervical sagittal alignment on cervical CT radiographs of asymptomatic persons. *Journal of Korean Neurosurgical Society*, *53*(6), 356–359. https://synapse.koreamed.org/articles/1161281

Parr, J. C., Miller, M. E., Colombi, J. M., Kabban, C. M. S., & Pellettiere, J. A. (2015). Development of a side-impact (Gy) neck injury criterion for use in aircraft and vehicle safety evaluation. *IIE Transactions on Occupational Ergonomics and Human Factors*, *3*(3-4), 151–164.

Philippens, M., Forbes, P. A., Wismans, J., DeWeese, R., & Moorcroft, D. (2011). *Neck injury criteria for side-facing aircraft seats* (Report No. DOT/FAA/AR-09/41). U.S. Department of Transportation.

Pintar, F. A., Schlick, M. B., & Yoganandan, N. (2010). Head-neck dynamics in frontal impact: Obtaining lower neck loads in PMHS. In *36th International Injury Biomechanics Research Workshop*. https://www-nrd.nhtsa.dot.gov/pdf/bio/Proceedings/2008_36/36-2.pdf

Pintar, F. A., Yoganandan, N., & Baisden, J. (2005). *Characterizing occipital condyle loads under high-speed head rotation* (No. 2005-22-0002). SAE Technical Paper. https://www.sae.org/publications/technical-papers/content/2005-22-0002/

Pintar, F. A., Yoganandan, N., & Maiman, D. J. (2010). *Lower cervical spine loading in frontal sled tests using inverse dynamics: Potential applications for lower neck injury criteria* (No. 2010-22-0008). SAE Technical Paper. https://www.sae.org/publications/technical-papers/content/2010-22-0008/

Prasad, P., & Daniel, R. (1984). A biomechanical analysis of head, neck, and torso injuries to child surrogates due to sudden torso acceleration. *SAE Transactions, 93*, 784–799. www.jstor.org/stable/44467191

Rooks, T., Logsdon, K., & McEntire, B. J. (2018). Evaluation of environmental sensors during laboratory direct and indirect head exposures. *Military Medicine*, *183*(3/4), 294–302. https://europepmc.org/article/med/29635599

Roush, G. C. (2010). *Finding cadaveric human head masses and center of gravity: A comparison of direct measurement to 3Ding* [Master's thesis, Wright State University]. https://rave.ohiolink.edu/etdc/view?acc_num=wright1282766380

SAE International. (2022). *Instrumentation for impact test part 1 - Electronic instrumentation* (SAE Standard J211/1_202208). SAE International. https://doi.org/10.4271/J211/1_202208

Yoganandan, N., Humm, J., Greenhalgh, P., & Somers, J. (2020). Lower neck injury criteria for THOR and Hybrid III dummies in rear impact. *Traffic Injury Prevention*, *21*(sup1), S176–S178. https://www.tandfonline.com/doi/full/10.1080/15389588.2020.1829925

U.S. ARMY AEROMEDICAL RESEARCH LABORATORY

FORT RUCKER, ALABAMA

Optimizing

HUMAN PROTECTION AND PERFORMANCE

since 1962

U.S. ARMY

FCC

MRDC